PHYSICAL REVIEW B VOLUME 26, NUMBER 2 15 JULY 1982

Semiempirical description of energy bands in nickel

F. Weling* and J. Callaway
Department of Physics and Astronomy, Louisiana State University, Baton Rouge, Louisiana 70803
(Received 11 January 1982)

The combined interpolation scheme is used to study energy bands in nickel. Parameters are determined by results of photoemission experiments. The Fermi surface is computed and compared with experiment. Explicit formulas are given for some bands along symmetry directions.

I. INTRODUCTION

For about three years it has been apparent that there is a serious discrepancy between calculated band structures of ferromagnetic nickel and the results of angularly resolved photoemission experiments.[1–5] On the other hand, there is reasonable agreement between calculations and the measured Fermi surface. We will not discuss in detail the possible reasons for the discrepancies which probably involve aspects of the electron-electron interaction which are not included in band calculations based on density-functional methods.[6–9] Our objective here is to obtain a semiempirical description of the nickel energy bands which agrees as reasonably as possible with the results of photoemission experiments, and is at the same time consistent with what is known about the nickel Fermi surface. Such a band structure would be useful in studying other properties of nickel; for example, magnetic excitations which are sensitive to some features of the band structure such as the exchange splitting.

In 1954 Slater and Koster[10] proposed an interpolation scheme for d bands in metals based on the tight-binding approximation. This has been extended by several authors to include a description of the s-p components of the band structure based on a few plane waves, and a pseudopotential.[11–14] We adopt here the "combined interpolation scheme" which is extensively described in Ref. 15. Spin-orbit coupling is neglected. Our procedures are discussed in Sec. II. In the course of this calculation we found that it was possible to obtain explicit formulas for the energy bands in certain directions in $\vec{k}$ space. These expressions, which are listed in tables, may be of use to others who desire to extend this work to other fcc materials. Section III discusses the fit to the paramagnetic band structure. The ferromagnetic bands are considered in Sec. IV. Some final discussion of an outstanding problem is contained in Sec. V.

II. FITTING PROCEDURE

The basis set for the combined interpolation scheme contains nine functions, five tight-binding d wave functions, and four orthogonalized plane waves.[11] The linear combination of atomic orbitals (LCAO) wave functions are linear combinations of the five atomic wave functions designated by their angular behavior as

$$|xy\rangle,\quad |yz\rangle,\quad |xz\rangle,\quad |x^2-y^2\rangle\ ,$$

and

$$\left|\frac{3z^2-r^2}{\sqrt{3}}\right\rangle$$

In practice the orthogonalized plane waves (OPW's) are simply replaced by plane waves

$$|\vec{k}+\vec{K}_i\rangle\ ,\quad i=1,\ldots,4$$

a pseudopotential is introduced, and in calculating LCAO-LCAO matrix elements, only nearest-neighbor interactions are taken into account. The Hamiltonian for the paramagnetic state of the metal is thus a 9×9 matrix consisting of an LCAO-LCAO, an OPW-OPW, and an LCAO-OPW block. We use the notation of Ref. 11 in discussing the Hamiltonian. The LCAO-LCAO matrix elements of the Hamiltonian depend on eight unknown parameters E_0, Δ, $A_1,\ldots,A_6$. E_0 and $E_0+\Delta$ are the diagonal matrix elements of the Hamiltonian with T_{2g} and E_g orbitals, respectively.

Thus

$$\langle\mu|\mathscr{H}|\mu\rangle=\begin{cases}E_0 \text{ if } \mu=xy;yz;xz,\\ E_0+\Delta \text{ if } \mu=x^2-y^2;\dfrac{3z^2-r^2}{\sqrt{3}}\end{cases}. \quad (1)$$

The quantities $A_1,\ldots,A_6$ are known as Fletcher parameters.

The OPW-OPW block depends on two pseudopotential coefficients V_{111} and V_{200} as well as in two parameters β and α relating, respectively, to the zero and to the dispersion of the free electron bands:

$$\langle\vec{k}+\vec{K}_i|\mathscr{H}|\vec{k}+\vec{K}_i\rangle = \beta+\alpha|\vec{k}+\vec{K}_i|^2, \quad i=1,\ldots,4. \quad (2)$$

The LCAO-OPW matrix elements are determined by two constants B_1 and B_2:

$$\langle\mu|\mathscr{H}|\vec{k}+\vec{K}_i\rangle \sim B_2 j_2(B_1|\vec{k}+\vec{K}_i|), \quad \mu=xy\ldots, \quad i=1,\ldots,4. \quad (3)$$

$j_2(x)$ is a spherical Bessel function. In order to be able to compute the paramagnetic bands of Ni, fourteen parameters have to be determined from experiments.

Our empirical band structure will be based on recent angle-resolved photoemission experiments which yield very accurate results for the energy bands of solids. We will determine the parameters of our Hamiltonain by fitting the experimental energy levels at certain symmetry points. This determination is greatly simplified by the use of analytic expressions for the energy levels. At $\vec{k}$ points of high symmetry the original 9×9 determinant can be brought into block-diagonal form by using basis functions, which transform like rows of the irreducible representations of the group of the $\vec{k}$ vector. Since the resulting blocks are generally 1×1 or 2×2 determinants, the computation of the energy eigenvalues is immediate. As an illustration we show how the expression for the W_2' level can be obtained. We use the notations of Burdick[16] and Hodges *et al.*[11,15] Using our set of nine wave functions we can form two basis functions of the representation W_2':

$$\phi_1=\tfrac{1}{2}|x^2-y^2\rangle+\frac{\sqrt{3}}{2}\left|\frac{3z^2-r^2}{\sqrt{3}}\right\rangle,$$
$$\phi_2=\tfrac{1}{2}(|\vec{k}+\vec{K}_1\rangle+|\vec{k}+\vec{K}_2\rangle-|\vec{k}+\vec{K}_3\rangle-|\vec{k}+\vec{K}_4\rangle). \quad (4)$$

Making the ansatz $\phi=a\phi_1+b\phi_2$ and evaluating the matrix elements of the Hamiltonian we obtain two energy levels,

$$E(W_2')=\frac{E_1+E_2}{2}\pm\left[\left[\frac{E_1-E_2}{2}\right]^2+V^2\right]^{1/2},$$

where

$$E_1=E_0+\Delta-4A_4,$$
$$E_2=\beta+80\alpha+V_{200}-2V_{111}, \quad (5)$$
$$V=-\tfrac{4}{5}B_2 j_2(\sqrt{80}B_1).$$

A comprehensive list of expressions for occupied energy levels is given in Table I. Some of the results have already been given by Ehrenreich and Hodges.[15] Some straightforward conclusions can be drawn from these equations. The first is that the energies X_5 and $W_{1'}$ should be identical, i.e.,

$$E(X_5)=E(W_{1'}). \quad (6)$$

Secondly, it is possible through elementary algebraic manipulations to derive a sum rule which can be used to determine the position of the K_2 energy level in terms of lower-lying levels,

$$K_2=\frac{1+\sqrt{2}}{4}(W_{1'}+X_2)+\frac{1-\sqrt{2}}{4}(\Gamma_{12}+\Gamma_{25'})+\tfrac{1}{2}(L_{31}+L_{32})-K_4. \quad (7)$$

This relation has proved helpful in our numerical calculations.

Using the same method we can also derive exact analytic expressions for some energy bands along high-symmetry directions. These expressions are listed in Table II. In cases where only parts of a band can be determined experimentally, e.g., the lower Λ_3 band given by Himpsel *et al.*,[4] these expressions can be used for extrapolation. Using precise Fermi-surface data, one could fit the point at which a given band crosses the Fermi level.

Once a paramagnetic band structure has been obtained, we can include the splitting to determine the ferromagnetic band structure. Since we are only interested in the overall features of the bands, we shall neglect the spin-orbit interaction. In accordance with previous band calculations, we assume that exchange effects on the OPW portion of the basis are negligible. The exchange-matrix elements are included only in the diagonal elements of the d-d block. This causes the d bands to split into majority (spin-up) and minority (spin-down) bands. Quite generally we allow the t_{2g} and e_g di-

TABLE I. Energy levels at symmetry points. The value of $E(L_1)$ given by Ehrenreich and Hodges is incorrect.

Point $\Gamma(000)$

$E(\Gamma_1)=\beta$

$E(\Gamma_{25'})=E_0-4A_1+8A_2$

$E(\Gamma_{12})=E_0+\Delta+4A_4-8A_5$

Point $X\ 2\pi/a(1,0,0)$

$$E(X_1)=H_-(E_1;E_2;V) \quad \text{where} \quad \begin{cases} E_1=\beta+64\alpha+V_{200} \\ E_2=E_0+\Delta-\frac{20}{3}A_4-\frac{8}{3}A_5 \\ V=\sqrt{(2/3)}B_2 j_2(8B_1), \end{cases}$$

$E(X_3)=E_0-4A_1-8A_2$

$E(X_2)=E_0+\Delta+4A_4+8A_5$

$E(X_5)=E_0+4A_1$

$E(X_{4'})=\beta+64\alpha-V_{200}$

Point $L\ 2\pi/a(\frac{1}{2},\frac{1}{2},\frac{1}{2})$

$$E(L_1)=H_-(E_1;E_2;V) \quad \text{where} \quad \begin{cases} E_1=\beta+48\alpha+V_{111} \\ E_2=E_0-8A_3 \\ V=\sqrt{(2/3)}B_2 j_2(\sqrt{48}B_1) \end{cases}$$

$$E(L_{31})=E_0+\frac{\Delta}{2}+2A_3-\tfrac{1}{2}[(\Delta-4A_3)^2+128A_6^2]^{1/2}$$

$E(L_{2'})=\beta+48\alpha-V_{111}$

$$E(L_{32})=E_0+\frac{\Delta}{2}+2A_3+\tfrac{1}{2}[(\Delta-4A_3)^2+128A_6^2]^{1/2}$$

Point $W\ 2\pi/a(1,\frac{1}{2},0)$

$$E(W_{2'})=H_-(E_1;E_2;V) \quad \text{where} \quad \begin{cases} E_1=E_0+\Delta-4A_4 \\ E_2=\beta+80\alpha+V_{200}-2V_{111} \\ V=\frac{4}{5}B_2 j_2(\sqrt{80}B_1) \end{cases}$$

$$E(W_3)=H_-(E_\perp;E_2;V) \quad \text{where} \quad \begin{cases} E_1=E_0-4A_2 \\ E_2=\beta+80\alpha-V_{200} \\ V=\dfrac{2\sqrt{2}}{5}B_2 j_2(\sqrt{80}B_1) \end{cases}$$

$$E(W_1)=H_-(E_1;E_2;V) \quad \text{where} \quad \begin{cases} E_1=E_0+\frac{16}{3}A_5+\frac{4}{3}A_4 \\ E_2=\beta+80\alpha+V_{200}+2V_{111} \\ V=\dfrac{2\sqrt{3}}{15}B_2 j_2(\sqrt{80}B_1) \end{cases}$$

$E(W_{1'})=E_0+4A_1$

Point $K\ 2\pi/a(\frac{3}{4},\frac{3}{4},0)$

$$E(K_3)=H_-(E_1;E_2;V) \quad \text{where} \quad \begin{cases} E_1=E_0+2\sqrt{2}A_1+2(1-\sqrt{2})A_2-2A_3 \\ E_2=\beta+2\alpha-V_{200} \\ V=\frac{4}{9}B_2 j_2(\sqrt{72}B_1) \end{cases}$$

$E(K_4)=E_0+\Delta+2A_4+4\sqrt{2}A_5$

$E(K_2)=E_0+2\sqrt{2}A_1+2(1-\sqrt{2})A_2+2A_3$

where $H_\pm(E_1;E_2;V)=\dfrac{E_1+E_2}{2}\pm\left[\left[\dfrac{E_1-E_2}{2}\right]^2+V^2\right]^{1/2}$

agonal elements to have different splittings. Thus

$$\begin{bmatrix} E_0^{\downarrow} \\ E_0^{\uparrow} \end{bmatrix} = E_0^{\text{param}} \pm \sigma_{t_{2g}} ,$$
$$\begin{bmatrix} E_0^{\downarrow}+\Delta^{\downarrow} \\ E_0^{\uparrow}+\Delta^{\uparrow} \end{bmatrix} = E_0^{\text{param}} + \Delta_{\text{param}} \pm \sigma_{e_g} , \tag{8}$$

where $2\sigma_{t_{2g}}$ ($2\sigma_{e_g}$) is the splitting of the $t_{2g}(e_g)$ levels. We assume that all the other parameters of our model are spin independent.

III. INTERPOLATION OF THE PARAMAGNETIC BANDS

The energy levels at symmetry points have been determined by Eberhardt and Plummer[5] (see also Refs. 4, 17, 18) and are given in Table III. Most of their data refer to averages of spin-up and spin-down levels and can readily be used to determine parameters of the paramagnetic band structure. In the case of L_3 and W_1' we use the expressions from Table I to determine the "experimental" average energy value:

$$\langle W_1' \rangle = W_{1\uparrow}' + \sigma_{t_{2g}} ,$$
$$\langle L_{32} \rangle \cong L_{32\uparrow} + \tfrac{1}{2}(\sigma_{t_{2g}} + \sigma_{e_g}) . \tag{9}$$

First we would like to discuss some of the difficulties which arose when we tried to fit the energy levels given by Eberhardt and Plummer. Inspection of the parametrized energy levels given in Table I indicates that it is particularly easy to obtain the constants E_0, β, Δ, $A_1, \ldots, A_6$ by fitting Γ_1, Γ_{12}, Γ_{25}', X_2, X_3, W_1', K_4, L_{31}, and L_{32}. If we use an exchange splitting of 0.31 eV as measured by Eastman *et al.*[17] for both e_g and t_{2g} states ($2\sigma_{t_{2g}} = 2\sigma_{e_g} = 0.31$) to obtain the "experimental" values of W_1' and L_{32} [Eq. (9)] it is not possible to fit the photoemission results (one would get an imaginary value for A_6. Although this is not necessarily a serious problem—slight readjustments of some experimental values within the error limits or a different value for the splitting will probably solve the problem—it raises some questions about the interpretation of the data. In view of this difficulty to fit the parametric energy levels and the fact that the most serious disagreement between theory and experiment concerns the value of X_2, it might be useful to examine more closely the relative position of X_2.

Eberhardt and Plummer[5] report X_2 to lie below Γ_{12} in contrast to theoretical predictions. Since (see Table I)

$$E(X_2) = E_0 + \Delta + 4A_4 + 8A_5 ,$$
$$E(\Gamma_{12}) = E_0 + \Delta + 4A_4 - 8A_5 , \tag{10}$$

we see that the relative position of the two levels depends on the sign of A_5. We think that A_5 is positive and that X_2 therefore should lie above Γ_{12}. A_5 can be expressed by the two center integrals defined by Slater and Koster (see Ehrenreich and Hodges[15]),

$$A_5 = -\tfrac{9}{16}(dd\delta) - \tfrac{3}{16}(dd\sigma) - \tfrac{1}{4}(dd\pi) . \tag{11}$$

The symmetry of the orbitals implies that $(dd\delta)$ and $(dd\sigma)$ are negative while $(dd\pi)$ is positive. Moreover, according to the conjecture of Heine[19] the ratio $\beta = |(dd\sigma)/(dd\pi)|$ should essentially be a function of the crystal structure. Zornberg[13] has found that $\beta \simeq 2$ with about 20% difference between β(Ni) and β(Cu). Thus

$$|(dd\pi)| \simeq \frac{|(dd\sigma)|}{2}$$

and

$$A_5 = -\tfrac{9}{16}|(dd\delta)| + \tfrac{1}{16}|(dd\sigma)| > 0 . \tag{12}$$

This is a strong albeit not a rigorous argument for the positiveness of A_5 and the fact that X_2 should be above Γ_{12}.

In view of the uncertainty of the value of X_2, a better approach is simply to exclude this level from our fit and to work with other data. In a second attempt we have used the values given for Γ_1, $\Gamma_{25'}$, Γ_{12}, X_1, X_3, L_1, L_{31}, $L_{2'}$, L_{32}, $W_{2'}$, W_3, W_1, $W_{1'}$, and K_3 and assumed that $2\sigma_{t_{2g}} = 2\sigma_{e_g} = 0.31$ to obtain "experimental" values for $\langle W_{1'} \rangle$ and $\langle L_{32} \rangle$ [Eq. (9)]. We have found that

$$\langle X_2 \rangle = -0.2094 , \tag{13}$$

measured in eV, is in reasonable agreement with the results of Wang and Callaway,[2] who found $\langle X_2 \rangle = -0.1830$ eV. When we used the results of this fit to compute the ferromagnetic bands, we obtained a correct value for E_F and for the magnetic number but in drawing the spin-down Fermi surface we found a small pocket near U. This is due to the fact that $\langle K_2 \rangle$ was lying too far below E_F.

Since no such pocket is found experimentally, we have to increase the value of $\langle K_2 \rangle$ in order to obtain qualitative agreement with the Fermi-surface results. For that purpose it was necessary

TABLE II. Analytic expressions for some energy bands.

ΓX direction $0 \le k \le 2\pi/a$

$$E(\Delta_2';k)=E_0-4A_1+8A_2\cos ka/2$$
$$E(\Delta_5;k)=E_0+4A_2-4(A_1-A_2)\cos ka/2$$
$$E(\Delta_2;k)=E_0+\Delta+4A_4-8A_5\cos ka/2$$

XW direction $0 \le k \le \pi/a$, $\mu=4ka/\pi$

$$E(Z_4;k)=H_-(E_1,E_2;V) \quad \text{where} \begin{cases} E_1=E_0-4A_2-4(A_1+A_2)\cos ka/2 \\ E_2=\beta+64\alpha+\alpha(\mu-8)^2-V_{200}[F_3(\mu,8,0)]^2 \\ V=-\dfrac{8\sqrt{2}(\mu-8)}{(\mu-8)^2+64}B_2 j_2\{B_1[(\mu-8)^2+64]^{1/2}\}F_3(\mu,8,0) \\ F_3(\mu,8,0)=\left[\dfrac{\mu}{\mu+0.001\cos ka/2\cos ka/3}\right]\dfrac{(\mu+8)(16-\mu)}{144} \end{cases}$$

$$E(Z_3;k)=H_-(E_1;E_2V)$$
$$E(Z_2;\mu)=E_0+4A_1 \quad \text{where} \begin{cases} E_1=E_0-4A_2+4(A_1+A_2)\cos ka/2 \\ E_2=\beta+64\alpha-V_{200}+\alpha\mu^2 \\ V=\dfrac{8\sqrt{2}\mu}{\mu^2+64}B_2 j_2[B_1(\mu^2+64)^{1/2}] \end{cases}$$

$\Gamma' L$ direction $0 \le k \le \pi/a$

$$E(\Lambda_3;k)=H_-(E_1;E_2;V) \text{ or } H_+(E_1;E_2;V), \text{ where} \begin{cases} E_1=E_0+4A_3-4(A_1-2A_2+A_3)\cos^2 ka/2 \\ E_2=E_0+\Delta+4(A_4-2A_5)\cos^2 ka/2 \\ V=-8/\sqrt{2}A_6\sin^2 ka/2 \end{cases}$$

ΓK direction $0 \le k \le 3\pi/2a$

$$E(\Sigma_2;k)=E_0+4A_3-4(A_1-A_2)\cos ka/2+4(A_2-A_3)\cos^2 ka/2$$
$$E(\Sigma_4;k)=E_0+\Delta-8A_5\cos ka/2+4A_4\cos^2 ka/2$$

where H_- and H_+ denote the lower and upper branch of two hybridized bands

$$H_\pm(E_1,E_2,V)=\frac{E_1+E_2}{2}\pm\left[\left[\frac{E_1-E_2}{2}\right]^2+V^2\right]^{1/2}$$

and where $j_2(x)$ is the spherical Bessel function

$$j_2(x)=\frac{3}{x^3}(\sin x-x\cos x)-\frac{\sin x}{x}$$

to make slight changes in the experimental values of Eberhardt and Plummer. We will fit the levels Γ_1, $\Gamma_{25'}$, Γ_{12}, X_3, X_4, L_{31}, L_2, L_{32}, $W_{2'}$, W_3, W_1, $W_{1'}$, K_3, and K_4. Equation (7) shows how the position of K_2 depends on the value of the other energy levels. Owing to the coefficient $(1-\sqrt{2})/4$ the dependence of K_2 on Γ_{12} and $\Gamma_{25'}$ is only weak and so we do not modify these values. Instead we adjust[20] the values of K_4, L_{32}, and X_2, measured in eV:

$$\begin{aligned} \langle K_4\rangle &= -0.4992\ , \\ \langle L_{32}\rangle &= -0.0551\ , \\ \langle X_2\rangle &= -0.1579\ . \end{aligned} \tag{14}$$

The value of $\langle X_2\rangle$ was chosen to be fairly close to

TABLE III. The energy levels at symmetry points as determined by Eberhardt and Plummer (units are electron volts).

Symmetry	Experiment[a] average[b]	Experiment[a] spin-up	Theory[c] average	Fit[d] average	Fit[d] spin-up	Fit[d] spin-down
Γ_1	-8.8 ± 0.2		-8.93		-8.8	-8.8
$\Gamma_{25'}$	-1.1 ± 0.2		-2.04		-1.3	-0.9
Γ_{12}	-0.4 ± 0.1		-0.92		-0.45	-0.35
X_1	-3.3 ± 0.2		-4.31	-3.24	-3.2789	-3.1942
X_3	-2.8 ± 0.2		-3.81		-3.0000	-2.6000
X_2	-0.85 ± 0.1		-0.18	-0.16*	-0.2079	-0.1079
X_5			0.02	0.05	-0.1500	0.2500
L_1	-3.6 ± 0.2		-4.63	-3.50	-3.6638	-3.3413
L_{31}	-1.3 ± 0.1		-2.07		-1.4035	-1.2045
$L_{2'}$	-1.0 ± 0.2		-0.40		-1.0000	-1.0000
L_{32}		-0.2 ± 0.1	-0.17	-0.06*	-0.2016	0.0994
$W_{2'}$	-2.6 ± 0.2		-3.59		-2.6422	-2.5583
W_3	-1.7 ± 0.2		-2.77		-1.8937	-1.5067
W_1	-0.65 ± 0.1		-1.00		-0.6998	-0.6000
$W_{1'}$		-0.15 ± 0.1	0.02		-0.1500	0.2500
K_1	-3.1 ± 0.2		-3.66	-2.70	-2.7549	-2.6549
K_1	-2.55 ± 0.1		-3.45	-2.40	-2.5787	-2.2119
K_3	-0.9 ± 0.2		-1.81		-1.0916	-0.7088
K_4	-0.45 ± 0.1		-0.77	-0.50*	-0.5492	-0.4492
K_2			-0.25	-0.09	-0.2881	0.1119

[a]W. Eberhardt and E. W. Plummer, Phys. Rev. B 21, 3245 (1980). The experimental Fermi energy was chosen as zero of energy.
[b]Average over the spin directions.
[c]C. S. Wang and J. Callaway, Phys. Rev. B 9, 4897 (1974).
[d]For the sake of clarity we only indicate the values found for the energy levels which have not been used for the fit. The values followed by an asterisk are the readjusted input values [Eq. (14)]. The fit accurately reproduced the experimental data which were used as input. The values are given relative to the experimental Fermi energy as for the column based on experiment.

the value found in our second fit [Eq. (13)]. The results of our interpolations are given in Table III. We notice that the predictions of the fit for X_1, L_1, K_{11}, and K_{12} are in good agreement with the photoemission results. The parameters used in the fit are given in Table IV.

IV. THE FERROMAGNETIC BAND STRUCTURE

In order to obtain the ferromagnetic band structure we now include the exhange splitting in our calculations. Since only the splitting of the d-bands seems appreciable, we simply replace the paramagnetic values of E_0 and Δ by their ferromagnetic values [Eqs. (8) and (9)]. All the other parameters have the values given in Table IV. We now can calculate the band structure and determine the Fermi surface. Our attempts to obtain a reasonable Fermi surface assuming that the t_{2g} and e_g levels have the same splitting have been unsuccessful. The principal difficulty is that a spin-down hole pocket associated with X_2 is obtained.

TABLE IV. Fit parameters for the nickel band structure.

$E_0=-0.95$	$\beta=-8.8$
$\Delta=0.059\,360$	$\alpha=0.204\,937$
$A_1=0.25$	$V_{111}=2.036\,977$
$A_2=0.106\,250$	$V_{200}=-0.387\,444$
$A_3=0.121\,385$	$B_1=0.480\,651$
$A_4=0.152\,923$	$B_2=12.870\,937$
$A_5=0.015\,131$	
$A_6=0.103\,386$	

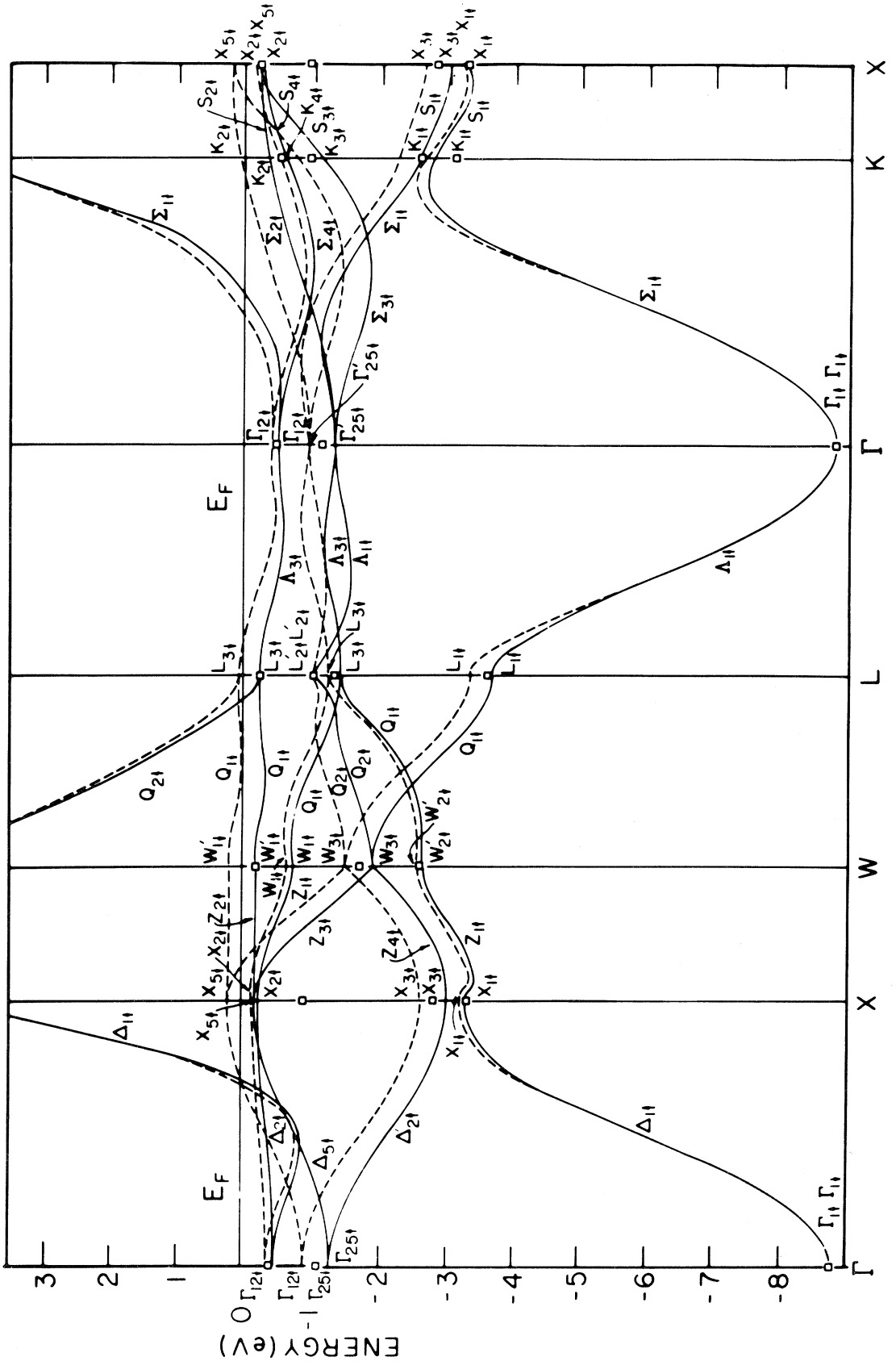

FIG. 1. Empirical-band structure of nickel along some symmetry lines. The solid lines indicate spin-up states, the dashed lines spin-down states. The experimental values are given by squares. The zero of energy is the experimental Fermi energy. Our Fermi energy is $E_F = 0.0548$ eV.

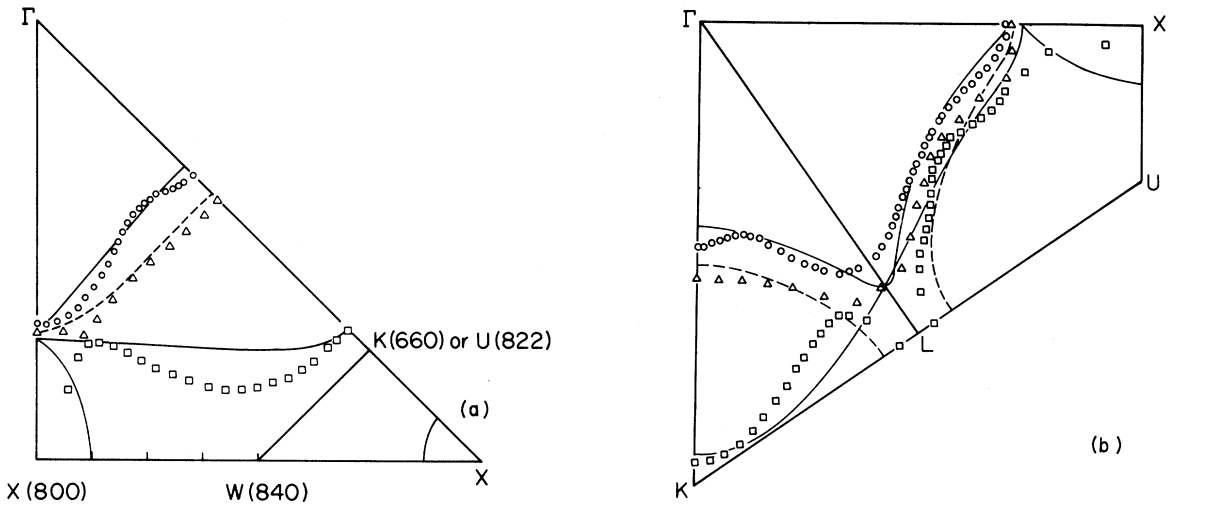

FIG. 2. (a) Fermi surface in a (100) plane. The solid lines are the calculated results for minority (↓) spin electrons, the dashed lines represent the majority (↑) spin surface. The points correspond to the Fermi surface obtained by a Kubic harmonic fit to the experimental observations by Stark (see Ref. 21). (b) Same as (a) but for a (110) plane.

A satisfactory fit has been obtained with the values

$$2\sigma_{t_{2g}}=0.4\ ,$$
$$2\sigma_{e_g}=0.1\ , \tag{15}$$

measured in eV. The values of E_0 and Δ are thus,

$$E_0^{\downarrow}=-0.75\ ,$$
$$E_0^{\uparrow}=-1.15\ , \tag{16}$$

$$E_0^{\downarrow}+\Delta_{\downarrow}=-0.84\ ,$$
$$E_0^{\uparrow}+\Delta_{\uparrow}=-0.94\ , \tag{17}$$

measured in eV. The band structure which we obtained is shown in Fig. 1. The Fermi energy (in eV) and the magnetic moment computed from these bands are given by

$$E_F=0.0548\ ,$$
$$\mu=0.5600\mu_B\ . \tag{18}$$

Since E_F is assumed to be zero in the fitting procedure, a small value in the final stage indicates that our procedure is reasonably consistent. The values of μ is in excellent agreement with experiment. The positions of the ferromagnetic energy levels are given in Table III. Figure 2 compares the Fermi surface determined from our bands with the experimental results of Stark and Tsui.[21–23] The agreement is good. This fit does not produce an $X_{2\downarrow}$ pocket. Some numerical results concerning the calculated Fermi surface are presented in Tables V and VI.

TABLE V. Extremal areas of Fermi-surface cross sections in atomic units.

Surface	Present results	Other values			
Small square ($sp\downarrow$)	0.85	0.84[a]	0.86[b]		0.90[d]
Large square ($sp\uparrow$)	1.09	1.24[a]	1.18[b]		1.15[d]
Γ centered $d_{\downarrow}$ sheet	1.95	2.20[a]	2.05[b]		
$X_{5\downarrow}$ pocket (1,0,0)	0.17	0.038[a]	0.0665[b]	0.0665[c]	

[a] C. S. Wang and J. Callaway, Phys. Rev. B 9, 4897 (1974).
[b] E. I. Zornberg, Phys. Rev. B 1, 244 (1970).
[c] D. C. Tsui, Phys. Rev. 164, 669 (1967).
[d] R. W. Stark (private communication).

TABLE VI. Comparison of $X_{5\downarrow}$ hole pocket dimensions in atomic units. The pocket is in the (100) plane.

	$k_{x\Gamma}$	k_{xW}	k_{xU}
Present calculation	0.256	0.118	0.125
a	0.195	0.077	0.076
b Parameters set IV	0.218	0.104	0.104
c	0.207	0.099	0.087

[a]C. S. Wang and J. Callaway, Phys. Rev. B 9, 4897 (1974).
[b]E. I. Zornberg, Phys. Rev. B 1, 244 (1970).
[c]D. C. Tsui, Phys. Rev. 164, 669 (1967).
[d]R. W. Stark (private communication).

V. DISCUSSION AND CONCLUSIONS

The principal uncertainty in the fitting procedure is the position of X_2; specifically, is there an $X_{2\downarrow}$ hole pocket? Failure to observe this pocket in de Haas–van Alphen effect measurements has led most investigators to conclude that this pocket does not exist, i.e., $X_{2\downarrow}$ is below E_F. This point of view has been adopted here. However, there is some contrary evidence[24,25] from studies of the angular variation of the magnetic anisotropy that there is a small $X_{2\downarrow}$ pocket. If this is so $X_{2\downarrow}$ must be almost exactly at the Fermi energy. In this case we do not require such a large difference between the t_{2g} and e_g splittings to obtain a fit; in fact, σ_{e_g} and $\sigma_{t_{2g}}$ would then be approximately equal.

This point has important implications. First-principles band calculations based on potentials obtained from a local-density approximation do not find much difference between the exchange splittings of states of these types. The fundamental reason for this is that local-density exchange-correlation potentials depend on the spin density of states of spin σ in the form $\rho_\sigma^{1/3}$ (times a function of density).[26] The cube root effectively smooths out much of the angular anisotropy of the spin density. Hence it is particularly important to establish whether or not σ_{e_g} and $\sigma_{t_{2g}}$ are substantially different to determine whether local-density potentials may give a quite poor description of the actual exchange interaction in transition metals.

Aside from this uncertainty, we see that it is, in fact, quite possible to obtain a band-structure fit to the energy levels determined by photoemission experiments which is at the same time in quite respectable agreement with the observed Fermi surface. We are presenting this semiempirical band structure in the hope that it will prove useful in the calculation of other properties of ferromagnetic nickel. At the same time, it must be cautioned that some difficulties may exist. The difference between the calculated bands of Ref. 2 and the experimental bands must result from many-body effects. Presumably the experimental observations locate the real part of the (complex) energy at which there is a pole of the one-body Green's function. However, since the lifetime of states well removed from the Fermi surface is probably rather short, there may be significant error introduced if one treats these empirical bands as sharp, i.e., neglects the imaginary part and assumes that the Green's function actually has poles at the energies of these bands. Further investigation will be required to determine whether these considerations seriously limit the utility of these bands. It is significant that their widths are not so large as to make them impossible to observe.

ACKNOWLEDGMENT

This research was supported in part by the Division of Materials Research of the U. S. National Science Foundation and in part by the Swiss National Science Foundation.

*Present address: Institute de Physique Theorique, Université de Lausanne, CH-1015 Lausanne, Switzerland.

[1]For surveys of current experimental and theoretical information concerning the band structure of ferromagnetic nickel, see J. Callaway, in *Physics of Transition Metals, 1980,* edited by P. Rhodes (Institute of Physics, London, 1981); D. E. Eastman, J. F. Janak, A. R. Williams, R. V. Coleman, and G. Wendin, J. Appl. Phys. 50, 7423 (1979).

[2]C. S. Wang and J. Callaway, Phys. Rev. B 15, 298 (1977).

[3]V. L. Moruzzi, J. F. Janak, and A. R. Williams, *Calculated Electronic Properties of Metals* (Pergamon, New York, 1978).

[4]F. J. Himpsel, J. A. Knapp, and D. E. Eastman, Phys. Rev. B 19, 2919 (1979).

[5]W. Eberhardt and E. W. Plummer, Phys. Rev. B 21, 3245 (1980).

[6]G. Treglia, F. Ducastelle, and D. Spanjaard (unpublished).

[7]L. Kleinman and F. Mednick, Phys. Rev. B 25, 1090 (1982)

[8]L. C. Davis and L. A. Feldkamp, Solid State Commun. 34, 141 (1980).

[9]A. Liebsch, Phys. Rev. Lett. 43, 1431 (1980).

[10]J. C. Slater and G. F. Koster, Phys. Rev. 94, 1498 (1954).

[11]L. Hodges, H. Ehrenreich, and N. D. Lang, Phys. Rev. 152, 505 (1966).

[12]F. M. Mueller, Phys. Rev. 153, 659 (1967).

[13]E. I. Zornberg, Phys. Rev. B 1, 244 (1970).

[14]J. Callaway and H. M. Zhang, Phys. Rev. B 1, 305 (1970).

[15]H. Ehrenreich and L. Hodges, Math. Comp. Phys. 8, 149 (1968).

[16]G. Burdick, Phys. Rev. 129, 138 (1963).

[17]D. E. Eastman, F. J. Himpsel, and J. A. Knapp, Phys. Rev. Lett. 40, 1514 (1978).

[18]E. Dietz, U. Gerhardt, and C. J. Maetz, Phys. Rev. Lett. 40, 892 (1978).

[19]V. Heine, Phys. Rev. 153, 673 (1967).

[20]With the splittings used below [Eq. (15)] the readjusted value of L_{32} corresponds to $L_{3\uparrow}=-0.18$ eV which is within the experimental error limits since $L_{3\uparrow,\text{expt}}=-0.45\pm0.1$ eV. the same holds true for K_4 since $K_{4,\text{expt}}=-0.45\pm0.1$ eV.

[21]R. W. Stark (private communication).

[22]R. W. Stark and D. C. Tsui, J. Appl. Phys. 39, 1056 (1968).

[23]D. C. Tsui, Phys. Rev. 164, 669 (1967).

[24]C. J. Tung, I. Said, and G. E. Everett, J. Appl. Phys. (in press).

[25]R. Gersdorf, Phys. Rev. Lett. 40, 344 (1978).

[26]U. von Barth and L. Hedin, J. Phys. C 5, 1629 (1972).